Chemistry of C-Trimethylsilyl-Substituted Heterocarboranes. 10. Syntheses, Structures, and Properties of Anionic Chromium(III) and Neutral Chromium(IV) Sandwiched Metallacarborane Complexes $\{1,1'$-*commo*-$Cr[2-(SiMe_3)-3-(R)-2,3-C_2B_4H_4]_2\}^-$ and $1,1'$-*commo*-$Cr[2,3-(SiMe_3)_2-2,3-C_2B_4H_4]_2$ (R = $SiMe_3$, Me, and H)

Aderemi R. Oki,† Hongming Zhang,† John A. Maguire,† Narayan S. Hosmane,*,† Hyekyeong Ro,‡ William E. Hatfield,‡ Michael Moscherosch,§ and Wolfgang Kaim§

Departments of Chemistry, Southern Methodist University, Dallas, Texas 75275, and University of North Carolina at Chapel Hill, Chapel Hill, North Carolina 27599, and Institut für Anorganische Chemie, Universität Stuttgart, Pfaffenwaldring 55, D-7000 Stuttgart 80, Germany

Received June 25, 1992

The reaction between $CrCl_3$ and the THF-solvated double salt $Na^+Li^+\{2-(SiMe_3)-3-(R)-2,3-C_2B_4H_4\}^{2-}$ [R = $SiMe_3$ (I), Me (II), and H (III)] in a molar ratio of 1:2 in benzene, followed by extraction and crystallization of the product from a solution of benzene and THF or TMEDA, produces the sandwiched paramagnetic species $Li(THF)_4\{1,1'$-*commo*-$Cr[2,3-(SiMe_3)_2-2,3-C_2B_4H_4]_2\}$ (IV), $Li(TMEDA)_2\{1,1'$-*commo*-$Cr[2-(SiMe_3)-3-(Me)-2,3-C_2B_4H_4]_2\}$ (V), and $Li(TMEDA)_2\{1,1'$-*commo*-$Cr[2-(SiMe_3)-2,3-C_2B_4H_5]_2\}$ (VI) as bright red-orange and air-sensitive crystalline solids in 77, 45, and 64% yields, respectively. The structural assignments of IV–VI, which were made in part by IR spectra and FAB mass spectral analysis, were confirmed by single-crystal X-ray diffraction studies. The structures reveal that the chromacarborane complexes are all ionic species in which the chromium metal is sandwiched by the two carborane ligands with the slight slippage of the metal toward the cage carbons. Complexes IV and VI crystallize in the monoclinic space group $C2/c$ and orthorhombic space group $Pccn$ with a = 19.276 (8) and 11.176 (5) Å, b = 14.662 (9) and 14.838 (6) Å, c = 18.085 (9) and 23.019 (9) Å, β = 100.53 (3) and 90.00°, V = 5025 (4) and 3817 (3) Å^3, and Z = 4 and 4, respectively. The final refinements of IV and VI converged at R = 0.081 and 0.069 and R_w = 0.110 and 0.059, respectively. Magnetic susceptibility and EPR spectra of IV indicate the presence of high-spin Cr(III) complexes. The chemical oxidation of IV with $PbCl_2$ produces the novel, diamagnetic, and neutral Cr(IV) sandwich complex $1,1'$-*commo*-$Cr[2,3-(SiMe_3)_2-2,3-C_2B_4H_4]_2$ (VII), as a dark-red and air-sensitive crystalline solid in 63% yield. Compound VII was characterized on the basis of ^1H, ^{11}B, and ^{13}C NMR spectra, IR and mass spectra, magnetic susceptibility, and also by X-ray diffraction. Compound VII crystallizes in the monoclinic space group $P2_1/n$ with the following unit cell parameters: a = 9.851 (3) Å, b = 13.813 (5) Å, c = 11.195 (5) Å, β = 95.66 (3)°, V = 1516 (1) Å^3, and Z = 4. Full-matrix least-squares refinements of VII converged at R = 0.047, and R_w = 0.068 for 1350 observed reflections.

Introduction

The π complexes formed between transition metals and *nido*-carborane anions have been the subject of extensive synthetic and structural investigations. The impetus for much of this work was the recognition by Hawthorne[1] of the similarities between the primary metal bonding orbitals of the cyclopentadienide ion, $[R_5C_5]^-$ (Cp^-), and the exopolyhedrally directed orbitals on the open faces of *nido*-dicarbollide ions, such as $[C_2R_2B_9H_9]^{2-}$ (R = H or a cage carbon substituent group). When bonding to a metal, the C_2B_3 pentagonal face of the carborane can function as a formal six-electron π donor, similar to Cp^-. The similarities in the ligating abilities of the two ligands have been repeatedly demonstrated in the syntheses and characterizations of a number of sandwich and half-sandwich metallacarborane complexes with a variety of different metal groups.[2] The most studied system has been the icosahedral metallacarboranes derived from the dianion, $[C_2R_2B_9H_9]^{2-}$. However, a fairly large body of data also exists for the pentagonal bipyramidal metallacarboranes, derived from the dianion, *nido*-$[2,3-C_2R_2B_4H_4]^{2-}$ (R = H or an exopolyhedral substituent group on the cage carbons).[2b,c] These metallacarboranes are not only interesting in terms of their structural, bonding, and reactivity patterns, they also can serve as precursors for the synthesis of extended multidecker clusters with potentially useful electrical and/or optical properties.[3] Although the analogy between the cyclopentadienide and carborane systems has proven to be a useful synthetic guide, the resulting organometallic compounds exhibit properties that seem to be characteristic of the particular ligand system. In general, the carborane dianions bond to metals more strongly than does Cp^-,[2b] for example, while $[Cp_2Cr]^+$ readily hydrolyzes, the corresponding $Cs[(C_2B_9H_{11})_2Cr]$ salt is quite air stable and can be recrystallized from hot aqueous solutions.[4] The structural distortion pattern exhibited by

† Department of Chemistry, Southern Methodist University.
‡ Department of Chemistry, University of North Carolina at Chapel Hill.
§ Institut Für Anorganische Chemie, Universität Stuttgart.

(1) Hawthorne, M. F.; Young, D. C.; Andrews, T. D.; Howe, D. V.; Pilling, R. L.; Pitts, A. D.; Reintjes, M.; Warren, L. F., Jr.; Wegner, P. A. *J. Am. Chem. Soc.* **1968**, *90*, 879 and references therein.

(2) For summaries see: (a) Hawthorne, M. F. In *The Chemistry of Boron and its Compounds*; Meutterties, E. L., Ed.; Wiley, New York, 1967. (b) Grimes, R. N. In *Comprehensive Organometallic Chemistry*; Wilkinson, G., Stone, F. G. A., Abel, E. W., Eds.; Pergamon: Oxford, 1982; Chapter 5.5. (c) Grimes, R. N. *Adv. Inorg. Chem. Radiochem.* **1983**, *26*, 55–117.

(3) Grimes, R. N. In *Electron Difficient Boron and Carbon Clusters*; Olah, G. A., Wade, K., Williams, R. E., Eds.; Wiley: New York, 1991; Chapter 11.

(4) Ruhle, H. W.; Hawthorne, M. F. *Inorg. Chem.* **1968**, *7*, 2279.

0276-7333/92/2311-4202$03.00/0

the transition metal sandwich complexes of the form $[(C_2R_2B_9H_9)_2M]^{n-}$ is different from that of the corresponding metallocenes. In metallacarboranes containing metals with six or fewer d electrons, the metal is centered above the C_2B_3 face of the carborane, while the more electron-rich metals are generally slipped toward the boron side of the pentagonal face of the carborane;[5] this type of distortion is not found in the simple metallocenes.[6] Extended Hückel calculations by Mingos and Forsyth have shown that the slippage in the electron-rich metallacarboranes relieves metal–carborane antibonding interactions that arise when higher energy, antibonding, MO's are occupied in such complexes.[7] The two ligand systems also support different metal oxidation states, with the metallocenes being the more restrictive. For example, the only nickelocene complex is $NiCp_2$, where nickel is formally in a 2+ state, while, in the corresponding $[Ni(C_2R_2B_9H_9)_2]^{n-}$ system, complexes with nickel in formal 2+, 3+, and 4+ states have been synthesized and structurally characterized.[8,9]

Next to the icosahedral complexes, the most studied system is that comprising the pentagonal bipyramidal metallacarboranes formed by the *nido*-$[2,3\text{-}(CR)_2B_4H_4]^{2-}$ ion. The majority of the structural data available pertain to mixed-olefin–carborane or mixed-metal complexes.[2b,c,3] An iron complex, $(Me_2C_2B_4H_4)_2FeH_2$, has been reported where the iron is centered between the parallel pentagonal faces of the carborane ligands and the hydrogens are, presumably, bonded directly to the iron but exert no steric influence.[10] A zirconium sandwich compound has also been reported[11] in which the zirconium, in a formal oxidation state of 4+, is bonded to a chloride ion and a THF molecule and η^5-bonded to the two carborane ligands, yielding a distorted tetrahedral arrangement about the zirconium similar to that found in $(\eta^5\text{-}C_5H_5)_2ZrCl_2$.[12] The dianionic $\{Y(Cl)(THF)[\eta^5\text{-}(SiMe_3)_2C_2B_4H_4]_2\}^{2-}$ was found to have a similar structure.[13] In contrast to the icosahedral system, the number of structural reports on simple transition metal complexes of the form $[M(C_2R_2B_4H_4)_2]^{n-}$ is quite limited; most of the structurally determined subicosahedral sandwich compounds are those containing main group metals.[14] The only reported structure of a *simple* pentagonal bipyramidal transition metal carborane sandwich complex is that of 1,1′-*commo*-$Cr[2,3\text{-}(SiMe_3)_2\text{-}2,3\text{-}C_2B_4H_4]_2$, described in our recent preliminary report.[15] This complex is unusual in that the chromium is in a formal 4+ oxidation state and is slightly slip distorted toward the carbon side of the C_2B_3 faces of the carborane ligands, thus showing a trend opposite to those observed in the structures of main group heterocarboranes. Here we report the details of the preparation, characterization, and structure of this complex, as well as that of the precursors, $\{1,1'\text{-}commo\text{-}Cr[2\text{-}(SiMe_3)\text{-}3\text{-}(R)\text{-}2,3\text{-}C_2B_4H_4]_2\}^-$ (R = $SiMe_3$, Me, and H) anion, along with the results of their magnetic studies and molecular orbital analyses.

Experimental Section

Materials. 2,3-Bis(trimethylsilyl)-2,3-dicarba-*nido*-hexaborane(8), 2-(trimethylsilyl)-3-methyl-2,3-dicarba-*nido*-hexaborane(8), and 2-(trimethylsilyl)-2,3-dicarba-*nido*-hexaborane(8) were prepared by the methods of Hosmane et al.[16,19] The double salt $Na^+(THF)Li^+[2\text{-}(SiMe_3)\text{-}3\text{-}(R)\text{-}2,3\text{-}C_2B_4H_4]^{2-}$ (R = $SiMe_3$, Me, and H) was prepared by the method described elsewhere.[20–22] Prior to use *N,N,N′,N′*-tetramethylethylenediamine (Aldrich), TMEDA, was distilled in vacuo, and stored over sodium metal. Purity was checked by IR and NMR spectra and boiling point measurements. Benzene, tetrahydrofuran (THF), and *n*-hexane were dried over $LiAlH_4$ and doubly distilled before use. All other solvents were dried over 4–8 mesh molecular sieves (Aldrich) and either saturated with dry argon or degassed before use. NaH (Aldrich) in a mineral oil dispersion, was washed repeatedly with dry *n*-pentane. *tert*-Butyllithium, BuLi (Aldrich), was used as received.

Spectroscopic Procedures. Proton, boron-11, and carbon-13 pulse Fourier transform NMR spectra, at 200, 64.2, and 50.3 MHz, respectively, were recorded on an IBM-200 SY multinuclear NMR spectrometer. The ^{11}B (115 MHz) NMR T_1 measurements were obtained from the Spectral Data Services, Inc., Champaign, IL. Infrared spectra were recorded on a Perkin-Elmer Model 283 infrared spectrophotometer and a Perkin-Elmer Model 1600 FT-IR spectrophotometer. Electron-spin paramagnetic resonance (EPR) spectra were recorded on a Bruker ESP 300 spectrometer in the X band. High-resolution electron-impact (HREI) and fast-atom bombardment (FAB) mass spectral determinations were performed at the Midwest Center for Mass Spectrometry, University of Nebraska-Lincoln, NE. Elemental analyses were obtained from Oneida Research Services, Inc., Whitesboro, NY.

Magnetic Susceptibility. Magnetic susceptibility measurements in the temperature range of 77–294 K were recorded for IV and VII by using a computer-controlled Faraday balance system that consisted of a Cahn 2000 electrobalance, a ANAC 4-in. electromagnet equipped with Lewis coils,[23] and a bipolar current-regulated power supply (George Associates, Berkeley, CA). A Tektronix 4052A computer and a Hewlett-Packard 3495 scanner with relay actuator were used for automated data collection. The samples were placed in polycarbonate capsules in an inert atmosphere box and sealed. These sealed capsules were transferred to the Faraday balance under a blanket of nitrogen, and the magnetic susceptibility measurements were made in a helium atmosphere. The calibration of the instrument, the procedures followed in the measurements, and the correction of the data for diamagnetism have been described previously.[24]

Synthetic Procedures. All experiments were carried out in Pyrex glass round-bottom flasks of 250-mL capacity, containing

(5) Wing, R. M. *J. Am. Chem. Soc.* **1968**, *90*, 4828.
(6) For a summary of the metal–carbon distances in the metallocenes and metallocenium ions, see: Haaland, A. *Acc. Chem. Res.* **1979**, *12*, 415.
(7) Mingos, D. M. P.; Forsyth, M. I. *J. Organomet. Chem.* **1978**, *146*, C37.
(8) Warren, L. F., Jr.; Hawthorne, M. F. *J. Am. Chem. Soc.* **1970**, *92*, 1157.
(9) (a) St. Clair, D.; Zalkin, A.; Templeton, D. H. *J. Am. Chem. Soc.* **1970**, *92*, 1173. (b) Churchill, M. R.; Gold, K. *J. Am. Chem. Soc.* **1970**, *92*, 1180. (c) Wing, R. M. *J. Am. Chem. Soc.* **1970**, *92*, 1187. (d) Hansen, F. V.; Hazell, R. G.; Hyatt, C.; Stucky, G. D. *Acta Chem. Scand.* **1973**, *27*, 1210.
(10) (a) Grimes, R. N. In *Advances in Boron and the Boranes*; Liebman, J. F., Greenberg, A., Williams R. E., Eds.; VCH: New York, 1988; Chapter 11 and references cited therein. (b) Pipal, J. R.; Grimes, R. N. *Inorg. Chem.* **1978**, *17*, 10. (c) Finster, D. C.; Grimes, R. N. *Inorg. Chem.* **1981**, *20*, 863. (d) Grimes, R. N.; Sinn, E.; Maynard, R. B. *Inorg. Chem.* **1980**, *19*, 2384.
(11) Siriwardane, U.; Zhang, H.; Hosmane, N. S. *J. Am. Chem. Soc.* **1990**, *112*, 9637.
(12) (a) Prout, K.; Cameron, T. S.; Forder, R. A.; Critchley, S. R.; Denton, B.; Rees, G. V. *Acta Crystallogr.* **1974**, *B30*, 2290. (b) Ronova, I. A.; Alekseev, N. V. *Zh. Strukt. Khim.* **1977**, *18*, 212.
(13) Oki, A. R.; Zhang, H.; Hosmane, N. S. *Organometallics* **1991**, *10*, 3964.
(14) Hosmane, N. S.; Maguire, J. A. *Adv. Organomet. Chem.* **1990**, *30*, 99.
(15) Oki, A. R.; Zhang, H.; Maguire, J. A.; Hosmane, N. S.; Ro, H.; Hatfield, W. E. *Organometallics* **1991**, *10*, 2996.
(16) Hosmane, N. S.; Sirmokadam, N. N.; Mollenhauer, M. N. *J. Organomet. Chem.* **1985**, *279*, 359.
(17) Hosmane, N. S.; Mollenhauer, M. N.; Cowley, A. H.; Norman, N. C. *Organometallics* **1985**, *4*, 194.
(18) Hosmane, N. S.; Maldar, N. N.; Potts, S. B.; Rankin, D. W. H.; Robertson, H. E. *Inorg. Chem.* **1986**, *25*, 1561.
(19) Hosmane, N. S.; Islam, M. S.; Burns, E. G. *Inorg. Chem.* **1987**, *26*, 3236.
(20) (a) Hosmane, N. S.; de Meester, P.; Siriwardane, U.; Islam, M. S.; Chu, S. S. C. *J. Chem. Soc., Chem. Commun.* **1986**, 1421. (b) Siriwardane, U.; Islam, M. S.; West, T. A.; Hosmane, N. S.; Maguire, J. A.; Cowley, A. H. *J. Am. Chem. Soc.* **1987**, *109*, 4600.
(21) Barreto, R. D.; Hosmane, N. S. *Inorg. Synth.* **1992**, *29*, 89–101.
(22) Hosmane, N. S.; Islam, M. S.; Pinkston, B. S.; Siriwardane, U.; Banewicz, J. J.; Maguire, J. A. *Organometallics* **1988**, *7*, 2340.
(23) Lewis, R. T. *Rev. Sci. Instrum.* **1971**, *42*, 31.
(24) Dobson, J. C.; Helms, J. H.; Doppelt, P.; Sullivan, B. P.; Hatfield, W. E.; Meyer, T. J. *Inorg. Chem.* **1989**, *28*, 2200.

magnetic stirring bars and fitted with high vacuum Teflon valves. Nonvolatile substances were manipulated in either a drybox or evacuable glovebags under an atmosphere of dry nitrogen. All known compounds among the products were identified by comparing their IR and ^{1}H NMR spectra with those of authentic samples.

Syntheses of Li(THF)$_4${1,1′-*commo*-Cr[2,3-(SiMe$_3$)$_2$-2,3-C$_2$B$_4$H$_4$]$_2$} (IV), Li(TMEDA)$_2${1,1′-*commo*-Cr[2-(SiMe$_3$)-3-(Me)-2,3-C$_2$B$_4$H$_4$]$_2$} (V), and Li(TMEDA)$_2${1,1′-*commo*-Cr-[2-(SiMe$_3$)-2,3-C$_2$B$_4$H$_5$]$_2$} (VI). A 6.7 mmol sample of Na$^+$(THF)Li$^+$[2,3-(SiMe$_3$)$_2$-2,3-C$_2$B$_4$H$_4$]$^{2-}$ (I), 8.71 mmol sample of Na$^+$(THF)Li$^+$[2,3-(SiMe$_3$)-3-(Me)-2,3-C$_2$B$_4$H$_4$]$^{2-}$ (II), or 9.5 mmol sample of Na$^+$(THF)Li$^+$[2-(SiMe$_3$)-2,3-C$_2$B$_4$H$_5$]$^{2-}$ (III) was allowed to react with anhydrous CrCl$_3$ [0.523 g (3.3 mmol), 0.689 g (4.35 mmol), and 0.752 g (4.75 mmol), respectively, when I, II, and III were used] in dry benzene (30 mL) at 0 °C for 5 h and then for 24 h at room temperature with constant stirring, during which time the solution became turbid and turned to reddish brown. At this point, the heterogeneous product mixture was filtered through a frit in vacuo, and the residue was washed repeatedly with a solvent mixture of anhydrous benzene (95%) and THF (5%), to collect a clear red-orange filtrate. The residue that remained on the frit after thorough washing was identified by qualitative analysis as a mixture of NaCl and LiCl salts and was therefore discarded. After removal of solvents from the filtrate in vacuo, a red-orange, air-sensitive solid remained in the flask. This solid was again dissolved in a minimum quantity of 1:1 mixture of THF and benzene and allowed to stand at room temperature for 6–7 days during which time bright red-orange crystals, identified as Li(THF)$_4${1,1′-*commo*-Cr[2,3-(SiMe$_3$)$_2$-2,3-C$_2$B$_4$H$_4$]$_2$} (IV; 2.0 g, 2.55 mmol; soluble in polar solvents; mp 210 °C dec) was obtained in 77% yield. Attempts to crystallize the other red-orange solids from 1:1 mixture of anhydrous benzene and THF were unsuccessful. However, addition of 4–5 mL of TMEDA to the solution resulted in the formation of platelike red-orange crystals, almost immediately. These crystals were later identified as the chromium(III) sandwich complex, Li(TMEDA)$_2${1,1′-*commo*-Cr[2-(SiMe$_3$)-3-(Me)-2,3-C$_2$B$_4$H$_4$]$_2$} (V; 1.2 g, 1.969 mmol, 45% yield; soluble in polar solvents, and slightly soluble in nonpolar solvents; mp 120 °C dec) or Li(TMEDA)$_2${1,1′-*commo*-Cr[2-(SiMe$_3$)-2,3-C$_2$B$_4$H$_5$]$_2$} (VI; 1.7 g, 3.04 mmol, 64% yield; soluble in polar solvents; mp 170 °C dec). Since the complexes IV–VI are all extremely sensitive to air and/or moisture, satisfactory microanalytical data could not be obtained even for single-crystal samples. Mass spectral analyses (low-resolution fast-atom bombardment (FAB) peak match): theoretical mass for the ion fragment of IV, [^{12}C$_{16}$^{1}H$_{44}$^{10}B$_1$^{11}B$_7$^{28}Si$_4$^{52}Cr]$^+$, *m/e* 487.2400, measured mass 487.3000; theoretical mass for the parent ion grouping of V, [^{12}C$_{24}$^{1}H$_{64}$^{14}N$_4$^{10}B$_2$^{11}B$_6$^{28}Si$_2$^{7}Li^{52}Cr]$^+$, [^{12}C$_{24}$^{1}H$_{64}$^{14}N$_4$^{10}B^{11}B$_7$^{28}Si$_2$^{7}Li^{52}Cr]$^+$, [^{12}C$_{24}$^{1}H$_{64}$^{14}N$_4$^{11}B$_8$^{28}Si$_2$^{7}Li^{52}Cr]$^+$, *m/z* 609.5370, 610.4900, and 611.4960, measured mass *m/e* 609.5370, 610.7500, and 611.7350, respectively; and theoretical mass for the ion fragment of VI, [^{12}C$_{10}$^{1}H$_{28}$^{10}B^{11}B$_7$^{28}Si$_2$^{52}Cr]$^+$, *m/e* 343.1929, measured mass *m/e* 343.1945. The infrared spectral data with selected assignments for IV–VI are presented in Table I.

Synthesis of 1,1′-*commo*-Cr[2,3-(SiMe$_3$)$_2$-2,3-C$_2$B$_4$H$_4$]$_2$ (VII). A 0.257 mmol sample of Li(THF)$_4${1,1′-*commo*-Cr[2,3-(SiMe$_3$)$_2$-2,3-C$_2$B$_4$H$_4$]$_2$} (IV) (0.2 g) was allowed to react with 0.137 mmol of anhydrous PbCl$_2$ (0.038 g) in dry, 1:1 mixture of THF/hexane (20 mL) at room temperature for 72 h, during which time the solution became turbid and turned to dark-red. After removal of THF and hexane from the heterogeneous solution in vacuo, the brown residue was heated to 120 °C, and the dark-red crystalline solid was sublimed from the reactor into a detachable U-trap that was held at 0 °C. The solid in the U-trap was later identified as neutral 1,1′-*commo*-Cr[2,3-(SiMe$_3$)$_2$-2,3-C$_2$B$_4$H$_4$]$_2$ (VII) (0.08 g, 0.162 mmol; 63% yield; mp 165 °C; soluble in both polar and nonpolar organic solvents). The residue that remained in the reactor after sublimation was identified by qualitative analysis as a mixture of elemental lead (Pb^0) and LiCl, and was therefore discarded. Since VII is *extremely air sensitive (turns green when exposed to air)* reproducible microanalytical data for the complex could not be obtained. Spectroscopic Data for VII: ^{1}H NMR (C$_6$D$_6$, relative to external Me$_4$Si) δ 3.24 [q (br), 8 H, basal and apical H$_t$, ^1J(^{1}H–^{11}B) = 142 Hz], 0.17 [s, 36 H, SiMe$_3$];

Table I. Infrared Absorptions (cm^{-1}, C$_6$D$_6$ vs C$_6$D$_6$)[a]

compound	absorption
IV	3092 (s), 3072 (s), 2923 (vvs), 2731 (s) [ν(C–H)], 2604 (ms), 2548 (ms) [ν(B–H)], 2324 (ws), 1461 (vs), 1379 (vs), 1343 (s), 1292 (s), 1248 (s), 1065 (ms), 1035 (s), 884 (s), 842 (s), 724 (vs), 671 (s)
V	2940 (vvs), 2850 (s), 2760 (s) [ν(C–H)], 2520 (vvs) [ν(B–H)], 1455 (m), 1440 (ms), 1280 (m), 1250 (s), 1200 (ms), 835 (vvs), 800 (sh), 750 (ms), 680 (ms), 620 (w), 480 (w), 430 (w)
VI	2950 (ms), 2850 (w), 2800 (wbr) [ν(C–H)], 2530 (ms) [ν(B–H)], 1450 (wbr), 1254 (sh), 1249 (s), 1090 (w), 1070 (w), 1025 (w), 830 (ms), 800 (s), 450 (w)
VII	3230 (m), 2960 (vs), 2900 (ms), 2850 (m) [ν(C–H)], 2580 (vvs), 2520 (vvs) [ν(B–H)], 2270 (vs), 1615 (m), 1450 (ms), 1405 (ms) [δ(CH)$_{asym}$], 1330 (s), 1250 (vs) [δ(CH)$_{sym}$], 1200 (vs), 1130 (s), 1095 (s), 1030 (w), 1020 (w), 985 (ms), 970 (m), 955 (m), 935 (ms), 900–800 (vvs, br) [ρ(CH)], 750 (s), 690 (s), 660 (m), 622 (m), 585 (m), 500 (vs, br), 345 (s)

[a] Legend: v = very, s = strong or sharp, m = medium, w = weak, sh = shoulder, and br = broad.

^{11}B NMR (C$_6$D$_6$, relative to external BF$_3$·OEt$_2$) δ −4.93 [d (br), 8 B, basal and apical BH, ^1J(^{11}B–^{1}H) = 141.3 Hz]; ^{13}C NMR (CDCl$_3$, relative to external Me$_4$Si) δ −1.08 [q, 12 C, SiMe$_3$, ^1J(^{13}C–^{1}H) = 119.4 Hz], −10.92 [s (br), 4 C, cage carbons (SiCB)]. The high-resolution electron-impact (HREI) mass spectrum of VII exhibited a parent ion grouping with the most abundant peak of exact mass 487.2706 (calcd mass, 487.2723) corresponding to [^{12}C$_{16}$^{1}H$_{44}$^{10}B^{11}B$_7$^{28}Si$_4$^{52}Cr]$^+$. The infrared spectral data with selected assignments for VII are presented in Table I.

Crystal Structure Analyses of Li(THF)$_4${1,1′-*commo*-Cr-[2,3-(SiMe$_3$)$_2$-2,3-C$_2$B$_4$H$_4$]$_2$} (IV), Li(TMEDA)$_2${1,1′-*commo*-Cr[2-(SiMe$_3$)-2,3-C$_2$B$_4$H$_5$]$_2$} (VI), and 1,1′-*commo*-Cr[2,3-(SiMe$_3$)$_2$-2,3-C$_2$B$_4$H$_4$]$_2$ (VII). Bright red-orange crystals of IV and VI were grown from 1:1 mixture of THF and benzene, and by further addition of TMEDA, respectively. Dark-red crystals of VII were grown by vaccum sublimation onto a Pyrex glass surface in a detachable U-trap. Since the crystals change to green upon brief exposure to air, they were introduced quickly into 0.5-mm Lindemann glass capillaries in a drybox, sealed with an epoxy resin, and mounted rapidly on a Nicolet R3m/V diffractometer. Pertinent crystallographic data are summarized in Table II. The final unit cell parameters were obtained by least-squares fit of 24 accurately centered reflections measured in the ranges of 15° < 2θ < 29°, 10° < 2θ < 20° and 13° < 2θ < 25° for IV, VI, and VII, respectively. Intensity data were collected at 230 K in the ranges of 3.5° ≤ 2θ ≤ 44.0°, 3.5° ≤ 2θ ≤ 40.0°, and 3.5° ≤ 2θ ≤ 42.0° for IV, VI, and VII, respectively. Three standard reflections, monitored after every 100 reflections, did not show any significant change in intensity during the data collection. These data were corrected for Lorentz and polarization effects. The semiempirical absorption correction method was applied, the minimum and maximum transmission factors for IV, VI, and VII are 0.7027 and 0.7580, 0.7107 and 0.7595, and 0.7027 and 0.7280, respectively. The structures were solved by heavy-atom methods stored in SHELXTL-Plus package.[25] All non-H atoms of IV, VI, and VII were refined anisotropically. Full-matrix least-squares refinements were performed for IV and VII, whereas structure of VI was refined by bloc-diagonal least-squares procedure. The bond lengths in solvated THF and Si–C(Me) bonds in the structure of IV were constrained due to disordered problems. Scattering factors, with corrections for anomalous dispersion for heavy atoms, were taken from the *International Tables for X-ray Crystallograpy*.[26] Cage-H atoms were located on DF maps for all three structures. Methyl- and methylene-H's in VI and VII were calculated. No attempts were made to locate H atoms of disordered methyl and methylene groups in structure of IV. The

(25) Sheldrick, G. M. Structure Determination Software programs; Nicolet Instrument Corp., Madison, WI, 1988.
(26) *International Tables For X-ray Crystallography*; Kynoch Press: Birmingham, U.K., 1974; Vol. IV.

Table II. Crystallographic Data[a] for IV, VI, and VII

	IV	VI	VII
formula	$C_{32}H_{76}O_4B_8Si_4CrLi$	$C_{22}H_{60}N_4B_8Si_2CrLi$	$C_{16}H_{44}B_8Si_4Cr$
fw	782.7	582.3	243.7
crystal system	monoclinic	orthorhombic	monoclinic
space group	$C2/c$	$Pccn$	$P2_1/n$
a, Å	19.276 (8)	11.176 (5)	9.851 (3)
b, Å	14.662 (9)	14.838 (6)	13.813 (5)
c, Å	18.085 (9)	23.019 (9)	11.195 (5)
β, deg	100.53 (2)	90.0	95.66 (3)
V, Å^3	5025 (4)	3817 (3)	1516 (1)
Z	4	4	4
D_{calcd}, g cm^{-3}	1.034	1.013	1.068
abs coeff, mm^{-1}	0.343	0.370	0.527
crystal dmns, mm	0.20 × 0.35 × 0.25	0.30 × 0.40 × 0.15	0.25 × 0.35 × 0.15
scan type	$\theta/2\theta$	$\omega/2\theta$	$\theta/2\theta$
scan sp in ω; min, max	5.0, 25.0	5.0, 25.0	5.0, 25.0
2θ range, deg	3.5–44.0	3.5–40.0	3.0–42.0
T, K	230	230	230
decay, %	0	0	0
data collected	3302	2124	1841
independent data	3057	2078	1619
obsd reflctns, $I > 3.0\sigma(I)$	1841	616 [$I > 2.0\sigma(I)$]	1350
parameters refined	245	170 [BLOCed]	145
GOF	2.54	1.33	3.20
R[b]	0.081	0.069	0.047
ωR	0.110	0.059	0.068
g[c]	0.0012	0.0004	0.0002
$Dr_{(max, min)}$, e/Å^3	0.28, −0.22	0.31, −0.32	0.37, −0.23

[a] Graphite-monochromatized Mo Kα radiation, λ = 0.710 73 Å. [b] $R = \sum||F_o| - |F_c||/\sum|F_o|$; $\omega R = [\sum\omega(F_o - F_c)^2/\sum\omega(F_o)^2]^{1/2}$. [c] $\omega = 1/[\sigma^2(F_o) + g(F_o)^2]$.

function minimized was $\sum\omega(|F_o| - |F_c|)^2$. In the final stages of refinement a weighting scheme was used (see Table II). The Cr atoms in all three structures were located at special positions. The cation of IV and the neutral molecule of VII have a center of symmetry, while cation of VI has a 2-fold symmetry. The ratios of largest parameter shifts to their estimated standard deviations were less than 0.01 in all three structures. The final atomic coordinates are listed in Table III. Selected bond lengths and bond angles are presented in Table IV.

Calculations. Molecular orbital calculations were carried out on $[(\eta^5\text{-}C_5H_5)_2Cr]^+$ (VIII) and the model compounds {1,1′-*commo*-Cr[2,3-$C_2B_4H_6$]$_2$}$^-$ (IX) and 1,1′-*commo*-Cr[2,3-$C_2B_4H_6$]$_2$ (X), using the unparameterized Fenske–Hall method.[27] The basis functions used were those generated by the numerical Xα atomic orbital program of Herman and Skillman,[28] used in conjunction with the Xα-to-Slater program of Bursten and Fenske.[29,30] Since the bond distances in IV and VII are the same within experimental error (see Table IV), the heavy-atom positions of IX and X were taken as those of VII and the relative positions of the hydrogen atoms in the carborane ligands were the MNDO-optimized ones calculated[31] for [*nido*-2,3-$C_2B_4H_6$]$^{2-}$. The Cr–C distances in VIII was taken from Haaland,[6] and the C–C and C–H bond distances were assumed to be 1.436 and 1.082 Å, respectively.

Results and Discussion

Synthesis. The reaction of $CrCl_3$ with the THF-solvated double salt Na^+Li^+\{2-($SiMe_3$)-3-(R)-2,3-$C_2B_4H_4$\}$^{2-}$ [R = $SiMe_3$ (I), Me (II), and H (III)] in a molar ratio of 1:2 in benzene produced the sandwiched ionic chromium complexes IV–VI. Isolation of $Li(THF)_4$\{1,1′-*commo*-Cr[2,3-($SiMe_3$)$_2$-2,3-$C_2B_4H_4$]$_2$\} (IV), in 77% yield, was ac-

Scheme I

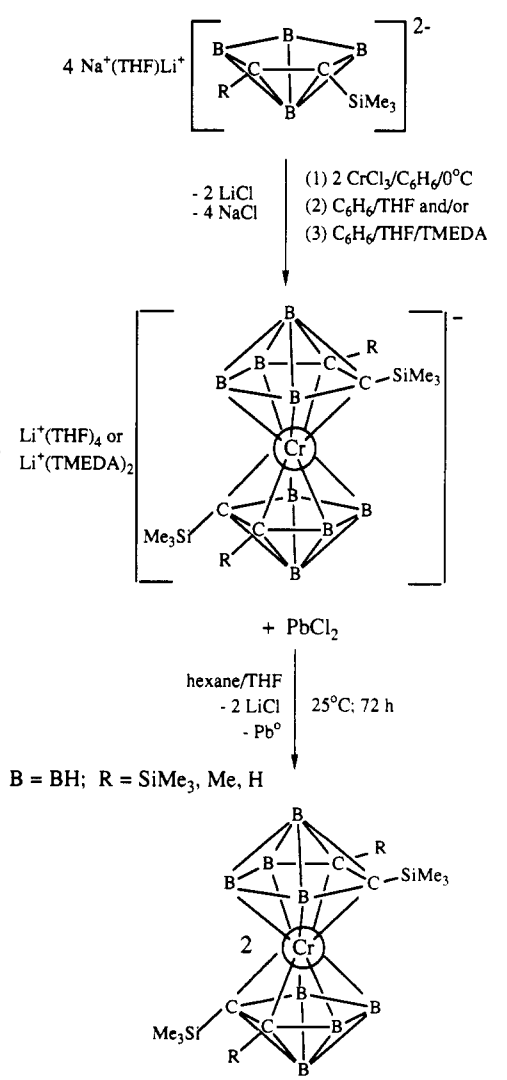

(27) Hall, M. B.; Fenske, R. F. *Inorg. Chem.* **1972**, *11*, 808.
(28) Herman, F.; Skillman, S. *Atomic Structure Calculations*; Prentice-Hall: Englewood, NJ, 1963.
(29) (a) Bursten, B. E.; Fenske, R. F. *J. Chem. Phys.* **1977**, *67*, 3138. (b) Bursten, B. E.; Jensen, R. J.; Fenske, R. E. *J. Chem. Phys.* **1978**, *68*, 3320.
(30) We wish to thank Prof. M. B. Hall, Texas A&M University, for furnishing a copy of this program.
(31) Maguire, J. A.; Ford, G. P.; Hosmane, N. S. *Inorg. Chem.* **1988**, *27*, 3354.

Table III. Atomic Coordinates (×10⁴) and Equivalent Isotropic Displacement Coefficients (Å² × 10³) for IV, VI, and VII

		Compound IV		
Cr	2500	2500	0	69 (1)
Si(1)	3773 (1)	1195 (2)	1371 (2)	135 (1)
Si(2)	3462 (2)	699 (2)	−788 (2)	158 (2)
C(1)	2975 (4)	1346 (5)	644 (5)	87 (3)
C(2)	2859 (4)	1146 (5)	−190 (5)	96 (3)
B(3)	2044 (7)	1221 (8)	−546 (7)	128 (5)
B(4)	1639 (5)	1436 (8)	120 (8)	124 (5)
B(5)	2261 (6)	1504 (8)	877 (6)	111 (5)
B(6)	2306 (6)	580 (7)	313 (7)	115 (5)
C(7)	3492 (6)	1483 (8)	2301 (4)	232 (9)
C(8)	4113 (6)	−27 (5)	1406 (6)	200 (7)
C(9)	4502 (4)	2006 (7)	1211 (7)	351 (14)
C(10)	3014 (7)	898 (8)	−1803 (4)	301 (14)
C(11)	4340 (5)	1331 (8)	−594 (8)	331 (17)
C(12)	3622 (7)	−572 (5)	−622 (6)	197 (8)
Li	0	680 (21)	2500	147 (12)
O(13)	438 (3)	−49 (4)	1868 (3)	120 (3)
C(14)	250 (7)	−209 (9)	1125 (4)	160 (8)
C(15)	697 (8)	−861 (10)	861 (6)	150 (7)
C(16)	1224 (7)	−1064 (9)	1502 (8)	200 (9)
C(17)	1001 (11)	−586 (16)	2105 (7)	399 (24)
C(14*)[b]	109 (8)	−851 (10)	1690 (20)	100 (12)
C(15*)[b]	550 (11)	−1495 (13)	1405 (26)	236 (39)
C(17*)[b]	1116 (6)	−189 (12)	1807 (19)	112 (15)
O(18)	706 (4)	1485 (5)	3107 (4)	158 (4)
C(19)	1238 (8)	1905 (14)	2852 (10)	407 (24)
C(20)	1765 (7)	2239 (12)	3449 (13)	277 (14)
C(21)	1480 (12)	2084 (15)	4113 (8)	341 (19)
C(22)	814 (11)	1659 (18)	3851 (6)	456 (27)
		Compound VI		
Cr	2500	2500	1414 (1)	56 (1)
Si	3392 (6)	773 (4)	2507 (3)	82 (3)
C(1)	2634 (20)	1186 (11)	1856 (7)	55 (9)
C(2)	1386 (18)	1490 (13)	1825 (9)	75 (10)
B(3)	928 (22)	1637 (17)	1197 (11)	88 (13)
B(4)	2096 (23)	1394 (15)	797 (9)	78 (12)
B(5)	3095 (21)	1103 (13)	1237 (10)	52 (10)
B(6)	1716 (25)	682 (16)	1372 (11)	82 (11)
C(7)	3487 (13)	−440 (12)	2491 (8)	127 (11)
C(8)	2597 (23)	1087 (10)	3170 (6)	136 (10)
C(9)	4882 (16)	1256 (13)	2529 (8)	181 (14)
Li	7500	2500	−109 (14)	59 (11)
N(1)	7161 (15)	1283 (10)	355 (7)	65 (8)
N(2)	5876 (14)	2288 (11)	−547 (8)	71 (8)
C(10)	6130 (25)	977 (15)	83 (9)	125 (16)
C(11)	5444 (21)	1563 (17)	−212 (12)	172 (19)
C(12)	6938 (13)	1401 (10)	979 (7)	79 (8)
C(13)	8092 (18)	585 (12)	311 (8)	115 (12)
C(14)	5042 (16)	2991 (13)	−565 (7)	104 (11)
C(15)	6043 (16)	1975 (13)	−1133 (8)	169 (15)
		Compound VII		
Cr	0	0	0	335 (4)
Si(1)	23509 (15)	−8755 (11)	26431 (14)	452 (6)
Si(2)	−15906 (16)	−14130 (12)	22974 (15)	508 (6)
C(1)	9016 (47)	−1389 (33)	18613 (43)	320 (18)
C(2)	−6144 (50)	−3385 (36)	17581 (44)	349 (18)
B(3)	−14651 (72)	5723 (51)	13184 (59)	492 (25)
B(4)	−2967 (68)	14488 (49)	11026 (64)	493 (25)
B(5)	12135 (72)	9117 (43)	14245 (58)	429 (24)
B(6)	−939 (65)	7577 (47)	24053 (65)	479 (25)
C(7)	38452 (60)	−570 (45)	30021 (72)	801 (30)
C(8)	19073 (70)	−13611 (50)	40924 (55)	732 (28)
C(9)	28519 (59)	−18375 (41)	16154 (57)	575 (23)
C(10)	−32513 (58)	−14820 (53)	13441 (60)	726 (27)
C(11)	−19203 (72)	−11817 (54)	38834 (59)	833 (31)
C(12)	−7341 (64)	−25810 (43)	20985 (66)	734 (28)

[a] Equivalent isotropic U defined as one-third of the trace of the orthogonalized U_{ij} tensor. [b] C(14*), C(15*), and C(17*), with 20% occupancy, are disordered positions of C(14), C(15), and C(17), respectively.

complished by recrystallization from a 1:1 mixture of benzene and THF. On the other hand, the addition of a small quantity of TMEDA to the 1:1 benzene/THF mixture was required to yield the crystals of Li(TMEDA)$_2$-{1,1′-*commo*-Cr[2-(SiMe$_3$)-3-(Me)-2,3-$C_2B_4H_4]_2$} (V) and Li(TMEDA)$_2${1,1′-*commo*-Cr[2-(SiMe$_3$)-2,3-$C_2B_4H_5]_2$} (VI), in 45 and 64% yields, respectively (see Experimental Section and Scheme I). Complexes IV–VI are all bright red-orange and air-sensitive crystalline solids whose yields were not improved when the reactions are carried out in anhydrous THF or *n*-hexane solvent alone. The chemical oxidation of IV with anhydrous $PbCl_2$ in a molar ratio 2:1 in dry hexane/THF solution produced the neutral chromium(IV) sandwich complex, 1,1′-*commo*-Cr[2,3-(SiMe$_3$)$_2$-2,3-$C_2B_4H_4]_2$ (VII), as dark-red, sublimable, and air-sensitive crystalline solid in 63% yield along with elemental lead (Pb^0) (see Scheme I).

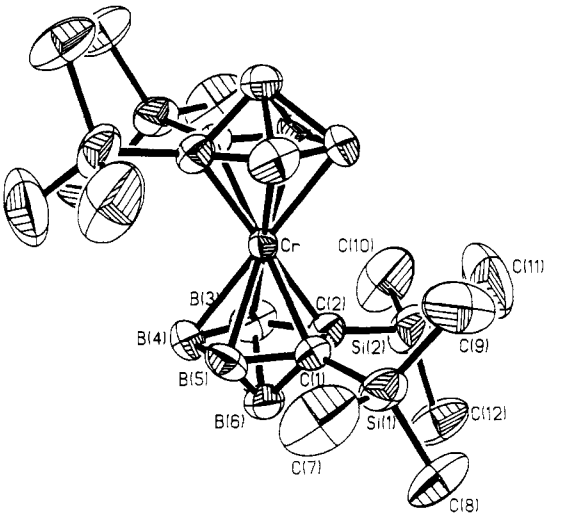

Figure 1. Perspective view of {1,1′-*commo*-Cr[2,3-(SiMe$_3$)$_2$-2,3-$C_2B_4H_4]_2$}$^-$ anion of IV showing the atom numbering scheme with thermal ellipsoids, drawn at the 25% probability level. The cage H's and the $Li^+(THF)_4$ cation are omitted for clarity.

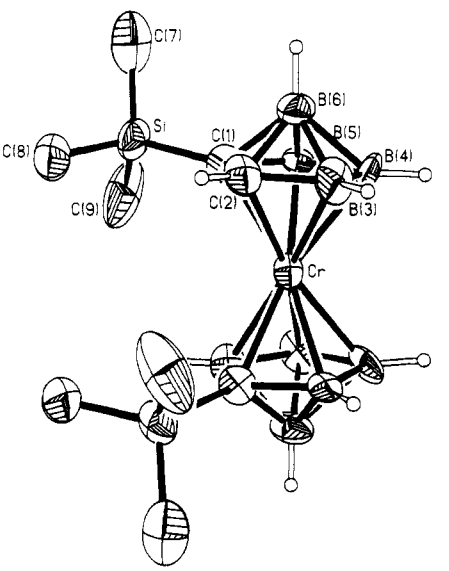

Figure 2. Perspective view of {1,1′-*commo*-Cr[2-(SiMe$_3$)-2,3-$C_2B_4H_5]_2$}$^-$ anion of VI showing the atom numbering scheme with thermal ellipsoids, drawn at the 40% probability level. The methyl H's and the $Li^+(TMEDA)_2$ cation are omitted for clarity.

Characterization. All compounds were characterized by infrared spectroscopy and mass spectrometry (see Table I and supplementary Table S-1). Complexes IV, VI, and VII were also characterized by single-crystal X-ray diffraction (see Tables II–IV and Figures 1–4). However, the structural analysis of V was incomplete due to severe

Table IV. Bond Lengths (Å) and Bond Angles (deg) for IV, VI, and VII

Bond Lengths

Compound IV

Cr–Cnt	1.777	C(2)–B(6)	1.734 (15)	Cr–C(1)	2.160 (7)	B(3)–B(4)	1.582 (20)
Cr–C(2)	2.151 (8)	B(3)–B(6)	1.806 (17)	Cr–B(3)	2.225 (12)	B(4)–B(5)	1.649 (15)
Cr–B(4)	2.317 (11)	B(4)–B(6)	1.784 (15)	Cr–B(5)	2.264 (11)	B(5)–B(6)	1.708 (16)
C(1)–C(2)	1.513 (12)	Si(1)–C(1)	1.845 (7)	C(1)–B(5)	1.529 (14)	Si(2)–C(2)	1.845 (10)
C(1)–B(6)	1.733 (13)	Li–O(13)	1.875 (18)	C(2)–B(3)	1.590 (15)	Li–O(18)	1.976 (20)

Compound VI

Cr–Cnt	1.771	B(3)–B(6)	1.716 (36)	Cr–B(3)	2.230 (25)	B(5)–B(6)	1.692 (36)
Cr–C(2)	2.166 (20)	B(4)–B(6)	1.745 (33)	Cr–B(5)	2.215 (20)	Li–N(2)	2.099 (22)
Cr–B(4)	2.216 (22)	Li–N(1)	2.132 (22)	Si–C(7)	1.804 (19)	N(1)–C(12)	1.467 (23)
Si–C(1)	1.828 (19)	N(1)–C(10)	1.388 (31)	Si–C(9)	1.814 (19)	N(2)–C(11)	1.410 (31)
Si–C(8)	1.826 (18)	N(1)–C(13)	1.471 (25)	C(1)–B(5)	1.520 (29)	N(2)–C(15)	1.439 (25)
C(1)–C(2)	1.468 (30)	N(2)–C(14)	1.399 (25)	C(2)–B(3)	1.548 (32)		
C(1)–B(6)	1.689 (33)	C(10)–C(11)	1.344 (35)	B(3)–B(4)	1.638 (35)		
C(2)–B(6)	1.631 (32)	Cr–C(1)	2.204 (16)	B(4)–B(5)	1.568 (33)		

Compound VII

Cr–Cnt	1.809	C(2)–Si(2)	1.899 (5)	Cr–C(1)	2.192 (5)	B(3)–B(4)	1.704 (10)
Cr–C(2)	2.167 (5)	B(3)–B(6)	1.745 (9)	Cr–B(3)	2.304 (7)	B(4)–B(5)	1.670 (9)
Cr–B(4)	2.384 (7)	B(4)–B(6)	1.738 (10)	Cr–B(5)	2.276 (6)	B(5)–B(6)	1.786 (10)
C(1)–C(2)	1.512 (7)	Si(1)–C(7)	1.868 (6)	C(1)–B(5)	1.571 (8)	Si(1)–C(8)	1.847 (7)
C(1)–B(6)	1.727 (8)	Si(1)–C(9)	1.856 (6)	C(1)–Si(1)	1.896 (5)	Si(2)–C(10)	1.865 (6)
C(2)–B(3)	1.564 (8)	Si(2)–C(11)	1.864 (7)	C(2)–B(6)	1.734 (8)	Si(2)–C(12)	1.844 (6)

Bond Angles

Compound IV

Cnt–Cr–Cnt[a,b]	180	C(1)–B(6)–B(4)	94.3 (7)	C(2)–C(1)–B(5)	109.1 (6)	C(1)–B(6)–B(5)	52.8 (6)
Si(1)–C(1)–B(5)	119.8 (6)	B(3)–B(6)–B(4)	52.3 (7)	C(2)–C(1)–B(6)	64.2 (6)	B(3)–B(6)–B(5)	93.7 (7)
Si(1)–C(1)–B(6)	129.7 (6)	C(2)–B(6)–B(5)	92.1 (7)	Si(2)–C(2)–C(1)	131.2 (6)	C(1)–Si(1)–C(7)	105.6 (4)
B(5)–C(1)–B(6)	62.8 (6)	B(4)–B(6)–B(5)	56.3 (6)	C(1)–C(2)–B(3)	110.2 (8)	C(1)–Si(1)–C(9)	111.0 (4)
Si(2)–C(2)–B(3)	118.0 (7)	C(1)–Si(1)–C(8)	111.9 (4)	C(1)–C(2)–B(6)	64.1 (6)	C(2)–Si(2)–C(11)	110.7 (5)
Si(2)–C(2)–B(6)	130.6 (6)	C(2)–Si(2)–C(10)	106.7 (5)	C(2)–B(3)–B(4)	107.1 (9)	O(13)–Li–O(18)	109.8 (3)
B(3)–C(2)–B(6)	65.7 (7)	C(2)–Si(2)–C(12)	110.9 (5)	C(2)–B(3)–B(6)	61.0 (6)	O(13)–Li–O(18[b])	110.0 (3)
Cr–B(3)–B(6)	91.8 (6)	O(13)–Li–O(13[b])	110.5 (16)	B(3)–B(4)–B(5)	105.0 (8)	Li–O(13)–C(14)	129.7 (8)
B(4)–B(3)–B(6)	63.2 (7)	O(18)–Li–O(18[b])	106.7 (15)	B(5)–B(4)–B(6)	59.5 (6)	Li–O(13)–C(14*)	113.5 (14)
B(3)–B(4)–B(6)	64.6 (7)	Li–O(13)–C(17)	124.4 (8)	C(1)–B(5)–B(6)	64.5 (6)	Li–O(18)–C(19)	124.9 (9)
C(1)–B(5)–B(4)	108.5 (8)	Li–O(13)–C(17*)	133.5 (13)	C(1)–B(6)–C(2)	51.7 (5)		
B(4)–B(5)–B(6)	64.2 (7)	Li–O(18)–C(22)	129.3 (12)	C(2)–B(6)–B(3)	53.3 (6)		
C(1)–B(6)–B(3)	91.9 (7)	Si(1)–C(1)–C(2)	129.8 (6)	C(2)–B(6)–B(4)	93.0 (7)		

Compound VI

Cnt–Cr–Cnt[a,c]	175.3	B(3)–B(6)–B(4)	56.5 (14)	Si–C(1)–C(2)	125.7 (14)	C(1)–B(6)–B(5)	53.4 (13)
Si–C(1)–B(5)	125.8 (16)	C(2)–B(6)–B(5)	93.0 (16)	Si–C(1)–B(6)	132.4 (13)	B(3)–B(6)–B(5)	96.9 (17)
C(2)–C(1)–B(5)	107.6 (16)	C(1)–Si–C(7)	110.2 (8)	C(2)–C(1)–B(6)	61.7 (14)	C(1)–Si–C(8)	112.0 (9)
B(5)–C(1)–B(6)	63.4 (14)	C(7)–Si–C(8)	107.6 (8)	C(1)–C(2)–B(3)	113.8 (17)	C(1)–Si–C(9)	108.4 (9)
C(1)–C(2)–B(6)	65.8 (14)	C(7)–Si–C(9)	109.9 (8)	B(3)–C(2)–B(6)	65.3 (15)	C(8)–Si–C(9)	108.8 (10)
C(2)–B(3)–B(4)	103.3 (18)	B(4)–B(6)–B(5)	54.3 (14)	C(2)–B(3)–B(6)	59.7 (14)	N(1)–Li–N(2)	87.7 (6)
B(4)–B(3)–B(6)	62.6 (15)	N(1)–Li–N(1[c])	119.8 (17)	B(3)–B(4)–B(5)	105.4 (17)	N(1)–Li–N(2[c])	121.4 (6)
B(3)–B(4)–B(6)	60.9 (15)	N(2)–Li–N(2[c])	122.7 (18)	B(5)–B(4)–B(6)	61.2 (15)	C(10)–N(1)–C(12)	109.8 (15)
C(1)–B(5)–B(4)	109.9 (18)	C(10)–N(1)–C(13)	108.9 (16)	C(1)–B(5)–B(6)	63.2 (15)	C(12)–N(1)–C(13)	105.8 (14)
B(4)–B(5)–B(6)	64.6 (15)	C(11)–N(2)–C(14)	111.0 (16)	C(1)–B(6)–C(2)	52.4 (12)	C(11)–N(2)–C(15)	108.1 (17)
C(1)–B(6)–B(3)	95.8 (16)	C(14)–N(2)–C(15)	107.4 (15)	C(2)–B(6)–B(3)	55.0 (13)	N(1)–C(10)–C(11)	119.3 (20)
C(1)–B(6)–B(4)	94.8 (16)	N(2)–C(11)–C(10)	125.1 (22)	C(2)–B(6)–B(4)	95.5 (16)		

Compound VII

Cnt–Cr–Cnt[a,d]	180.0	C(1)–B(6)–C(2)	51.8 (3)	C(2)–C(1)–B(5)	111.5 (4)	C(1)–B(6)–B(3)	94.4 (4)
C(2)–C(1)–B(6)	64.3 (3)	C(2)–B(6)–B(3)	53.4 (3)	B(5)–C(1)–B(6)	65.3 (4)	C(1)–B(6)–B(4)	96.9 (5)
C(2)–C(1)–Si(1)	129.1 (3)	C(2)–B(6)–B(4)	97.1 (4)	B(5)–C(1)–Si(1)	118.5 (4)	B(3)–B(6)–B(4)	58.6 (4)
B(6)–C(1)–Si(1)	130.5 (4)	C(1)–B(6)–B(5)	53.1 (3)	C(1)–C(2)–B(3)	111.8 (4)	C(2)–B(6)–B(5)	92.8 (4)
C(1)–C(2)–B(6)	63.9 (3)	B(3)–B(6)–B(5)	98.3 (5)	B(3)–C(2)–B(6)	63.7 (4)	B(4)–B(6)–B(5)	56.5 (4)
C(1)–C(2)–Si(2)	130.2 (3)	C(1)–Si(1)–C(7)	108.4 (3)	B(3)–C(2)–Si(2)	117.2 (4)	C(1)–Si(1)–C(8)	111.6 (3)
B(6)–C(2)–Si(2)	133.5 (4)	C(7)–Si(1)–C(8)	106.3 (3)	C(2)–B(3)–B(4)	105.5 (5)	C(1)–Si(1)–C(9)	109.4 (2)
C(2)–B(3)–B(6)	62.9 (4)	C(7)–Si(1)–C(9)	108.3 (3)	B(4)–B(3)–B(6)	60.5 (4)	C(8)–Si(1)–C(9)	112.6 (3)
B(3)–B(4)–B(5)	104.7 (5)	C(2)–Si(2)–C(10)	107.5 (3)	B(3)–B(4)–B(6)	60.9 (4)	C(2)–Si(2)–C(11)	108.1 (3)
B(5)–B(4)–B(6)	63.2 (4)	C(10)–Si(2)–C(11)	109.2 (3)	C(1)–B(5)–B(4)	106.3 (5)	C(2)–Si(2)–C(12)	113.2 (3)
C(1)–B(5)–B(6)	61.5 (4)	C(10)–Si(2)–C(12)	105.8 (3)	B(4)–B(5)–B(6)	60.3 (4)	C(11)–Si(2)–C(12)	112.9 (3)

[a] Cnt stands for the centroid of C(1), C(2), ... B(5) ring. [b] Symmetry operator: 0.5 − *x*, 0.5 − *y*, −*z*. [c] Symmetry operator: 0.5 − *x*, 0.5 − *y*, *z*. [d] Symmetry operator: −*x*, −*y*, −*z*.

crystallographic disorder problems and, therefore, no X-ray data on this compound were included here. While the paramagnetism of the ionic species was determined on the basis of magnetic susceptibility measurements and EPR spectra obtained for IV, the diamagnetic VII, as confirmed by its effective magnetic moment (discussed in the following section), was also characterized by ^{1}H, ^{11}B, and ^{13}C NMR spectra (see Experimental Section).

NMR Spectra. The paramagnetism of the ionic complexes IV, V, and VI precluded obtaining useful NMR data. However, the neutral Cr(IV) complex, VII, exhibits a rather unusual NMR spectra. The ^{1}H and ^{13}C NMR

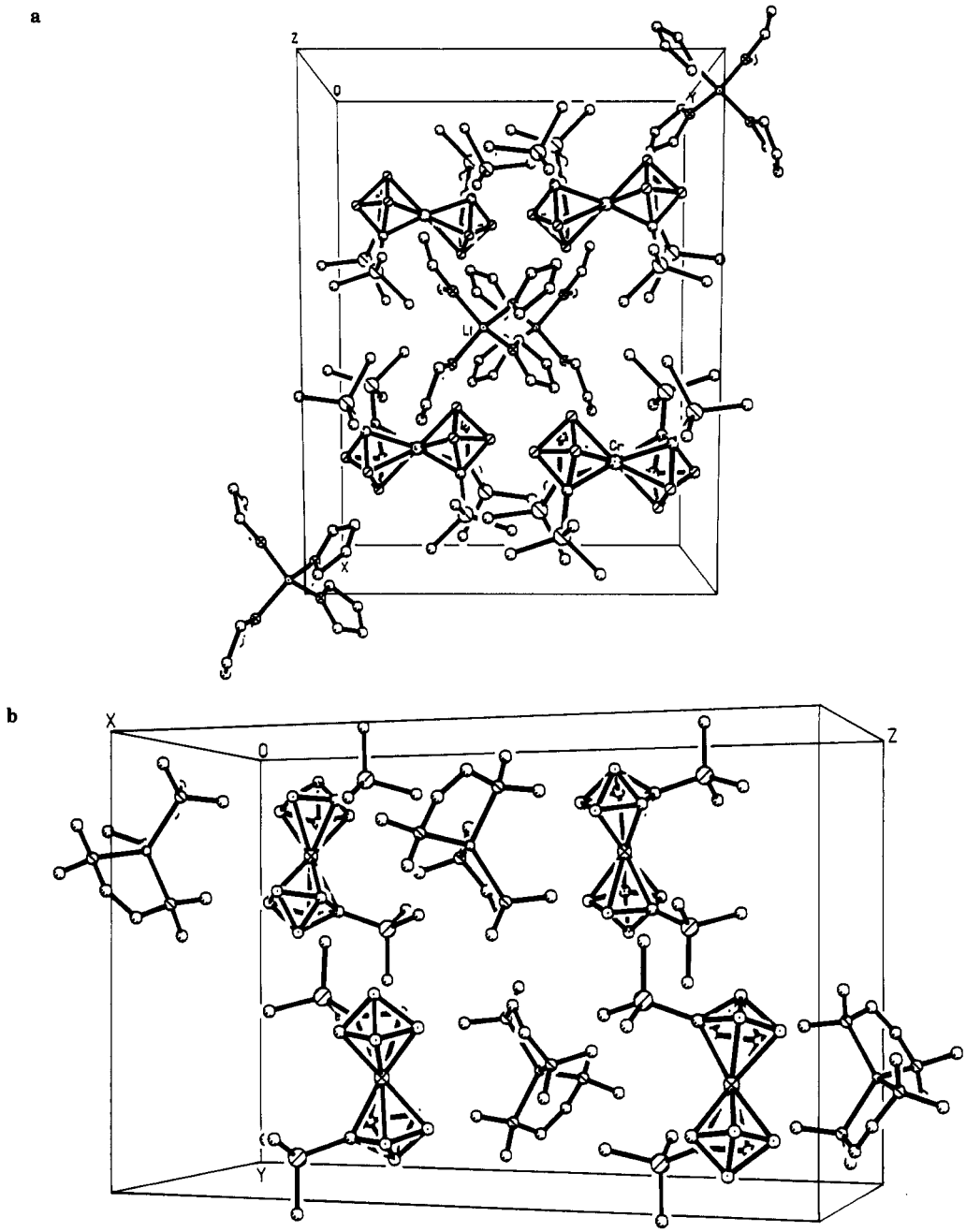

Figure 3. Packing diagrams showing both the cation and anions in the unit cells of (a) IV and (b) VI.

spectra of VII were consistent with the presence of all equivalent $SiMe_3$ groups. The ^{11}B NMR spectrum of this complex showed a single broad doublet at −4.93 ppm [$^1J(^{11}B-^1H)$ = 141.3 Hz, see Experimental Section]. Since the magnetic measurements on VII showed a very weak paramagnetic signal ($\chi = 2.0 \times 10^{-7}$ emu/g) and a carefully purified sample gave well-resolved NMR spectra, the complex is considered to be diamagnetic, and the weak paramagnetic signal could be due to an impurity arising from reaction of IV with the sample holder. Therefore, the presence of a single resonance in the proton-decoupled ^{11}B NMR spectra may not be due to a paramagnetic shift, but it could rather be the result of either a fluxional behavior of the complex, or the result of an accidental overlap of the apical and basal boron resonances, which has been previously observed in polyhedral borane chemistry.[2b] In an effort to obtain more information, ^{11}B (T_1) NMR measurements were made. The ^{11}B (T_1) NMR spectra of VII showed a single broad signal at −4.9 ppm, over a period of 1 μs to 5 ms with an inversion recovery of 0.99 ms. Thus, T_1 measurements were not helpful in clarifying the ^{11}B NMR spectra of VII. Since all of the previously reported heterocarboranes, derived from the dianions I–III, have been found to be stereochemically rigid on an NMR time scale, the single resonance in the ^{11}B NMR spectrum of VII is most likely due to an accidental overlap of its basal and apical boron resonances.[14,32] One of the interesting features of the NMR spectra of VII is that, in both the proton-coupled and proton-decoupled ^{13}C NMR spectra, the cage carbon resonance appears as a broad singlet at −10.92 ppm. This represents a significant upfield shift, by about 154 ppm, from that of the *nido*-carborane precursor,[21] indicating a strong shielding of the cage carbons on complexation with the chromium metal. However, such a strong shielding of the cage carbon resonance has not been observed in the ^{13}C NMR spectra of main group heterocarboranes.[14,32]

(32) Hosmane, N. S. *Pure Appl. Chem.* **1991**, *63*, 375 and references therein.

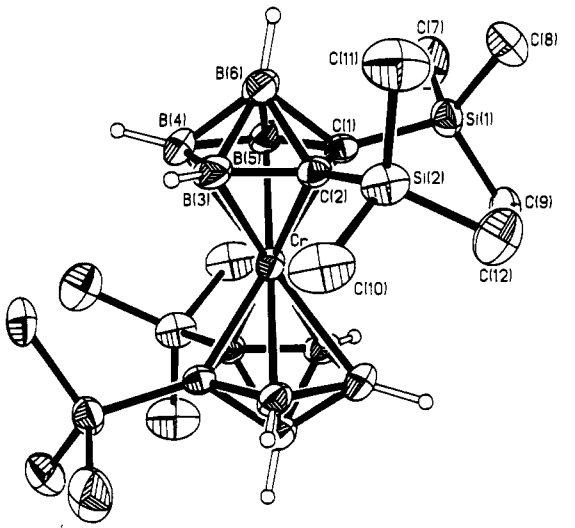

Figure 4. Perspective view of the Cr(IV) complex 1,1′-*commo*-Cr[2,3-(SiMe$_3$)$_2$-2,3-$C_2B_4H_4$]$_2$ (VII) with thermal ellipsoids drawn at the 40% probability level and showing the atom numbering scheme. The central Cr atom lies at a crystallographic center of symmetry. The silylmethyl H's are omitted for clarity.

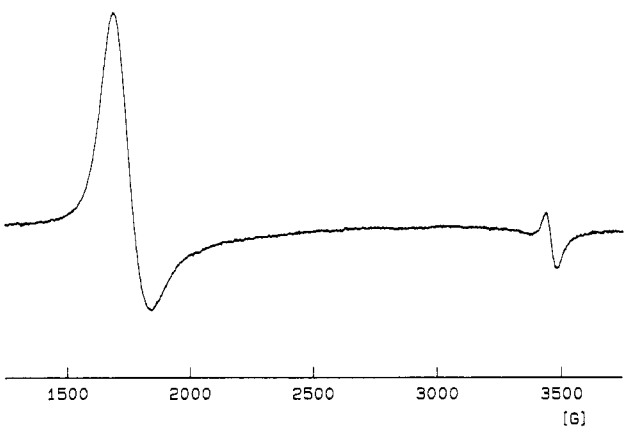

Figure 5. EPR spectrum of a powdered sample of IV at 100 K (ν = 9.621 72 GHz).

EPR Spectra. The low-temperature EPR spectrum of solid IV (Figure 5) exhibits the characteristic features of high-spin Cr(III)(d^3) centers with large zero-field splitting, D.[33,34] There is an unstructured $g_\parallel$-type signal at $g \approx 2$ (345.3 mT at 9.622 GHz, 2 mT peak-to-peak line width) and a $g_\perp$-type signal at $g \approx 4$ (176.0 mT at 9.622 GHz, 1.6 mT peak-to-peak line width). The latter signal shows a structuring at 4 K with three overlapping peaks separated by 2 × 2.4 mT.

Molecular orbital analysis of the model compound, $[Cr(C_2B_4H_6]^-$, shows that the chromium d^3 electrons occupy a set of three metal-centered orbitals much the same as would be encountered in an axially distorted octahedral environment (see below). Therefore, to a first approximation, the spin Hamiltonian for the octahedral environment can be used (eq 1).[35] This Hamiltonian yields four energy levels for

$$\mathcal{H} = g_\parallel \mu_B H_z + g_\perp \mu_B (H_x S_x + H_y S_y) + D[S_z^2 - \tfrac{1}{3}S(S+1)] \quad (1)$$

which the transitions, with $\Delta m_S = 1$, are

$$\Delta W(-\tfrac{3}{2} \rightarrow -\tfrac{1}{2}) = g\mu_B H - 2D \quad (2)$$

$$\Delta W(-\tfrac{1}{2} \rightarrow +\tfrac{1}{2}) = g\mu_B H \quad (3)$$

$$\Delta W(+\tfrac{1}{2} \rightarrow +\tfrac{3}{2}) = g\mu_B H + 2D \quad (4)$$

Only one transition, $\Delta W(-^1/_2 \rightarrow +^1/_2)$, is observed which suggests that $|D| > h\nu = 0.32$ cm^{-1}.[48]

In another approach to determining D,[50] the zero-field splitting can be estimated from the relationship

$$D = \tfrac{1}{2}\lambda(g_\parallel - g_\perp) \quad (5)$$

where $\lambda = 2\xi S$, and ξ is the spin–orbit coupling constant. According to the unresolved line at $g \approx 2$, the upper limit of $|g_\parallel - g_\perp|$ is about 0.012. This, together with a value of ξ = 273 cm^{-1} for Cr(III),[34] yields a $|D| < 0.55$ cm^{-1}. These limits indicate a value of D in the order of half a wavenumber. These rather large values of D would lead to transitions $\Delta W(-^3/_2 \rightarrow -^1/_2)$ and $\Delta W(+^1/_2 \rightarrow +^3/_2)$ that are outside the range of normal spectrometers. The two signals observed for the transition $\Delta W(-^1/_2 \rightarrow +^1/_2)$ are the result of the angular dependence of the g and D tensors in a powdered sample. This result can be compared to the values of $g_\parallel = 1.97$, $g_\perp = 2.02$, and $|D| = 1.5$ cm^{-1} reported for polycrystalline $(CH_3)_4N^+[Cr^{III}(C_2B_9H_{11})_2]^-$ at 80 K.[36]

The EPR results of IV are typical for chromium(III) (d^3) with rather large zero-field splitting in an environment similar to that found in a distorted octahedral ligand field.

Magnetic Susceptibility. The magnetic susceptibilities of IV and VII were measured in the temperature range 77 K to room temperature. The effective magnetic moment of IV is 3.93 μ_B at room temperature. This is a typical value for an $S = ^3/_2$ paramagnetic system. The magnetic data of IV follow the Curie law with a Curie constant of 1.933 and a g value of 2.03.

Compound VII, which had a d^2 electronic configuration, is nearly diamagnetic over the temperature range studied. The effective magnetic moment of 0.99 μ_B at room temperature is most probably due to impurities, such as unoxidized IV, or products of the reaction of VII with the sample holder. The singlet state of VII is consistent with the observation that the well-resolved ^{1}H, ^{11}B, and ^{13}C NMR spectra for this complex could be obtained (see Experimental Section).

Structure and Bonding. The crystal structures of IV, VI, and VII show chromacarborane cages that are almost identical (see Table IV and Figures 1–4). Inspection of Table IV shows that the chromium–cage atom bond distances in the three chromacarboranes are the same within experimental indetermination. All structures show that the chromiums are equally bonded to the pentagonal C_2B_3 faces of the two carborane ligands. The bonding faces of the carboranes are parallel to one another, giving rise to a C_{2h} symemtry for the $Cr(C_2B_4)_2$ cage. The Cr–C(cage) bond distances in IV, VI, and VII are shorter than those of 2.26 and 2.27 Å found in the corresponding icosahedral chromacarborane sandwich compound,[37] and about the same as the analogous distances of 2.179 Å reported by Grimes and co-workers[38] for 1-Cr(η^7-C_7H_7)-2,3-(C_2H_5)$_2$-2,3-$C_2B_4H_4$, as well as the average Cr–C bond distance of 2.169 Å found in chromocene.[39,40] A careful inspection of

(33) Symons, M. *Chemical and Biological Aspects of Electron Spin Resonance*; Van Nostrand Reinhold: New York, 1978; pp 140–142.
(34) Goodman, B. A.; Raynor, J. B. *Adv. Inorg. Chem. Radiochem.* **1970**, *13*, 135.
(35) Abragam, A.; Bleaney, B. *Electron Paramagnetic Resonance of Transition Metal Complexes*; Clarendon Press: Oxford, 1970; pp 427–433.
(36) Wiersema, R. J.; Hawthorne, M. F. *J. Am. Chem. Soc.* **1974**, *96*, 761.
(37) St. Clair, D.; Zalkin, A.; Templeton, D. H. *Inorg. Chem.* **1971**, *10*, 2587.
(38) Swisher, R. G.; Sinn, E.; Grimes, R. N. *Organometallics* **1984**, *3*, 599.
(39) Haaland, A. *Acc. Chem. Res.* **1979**, *12*, 415.

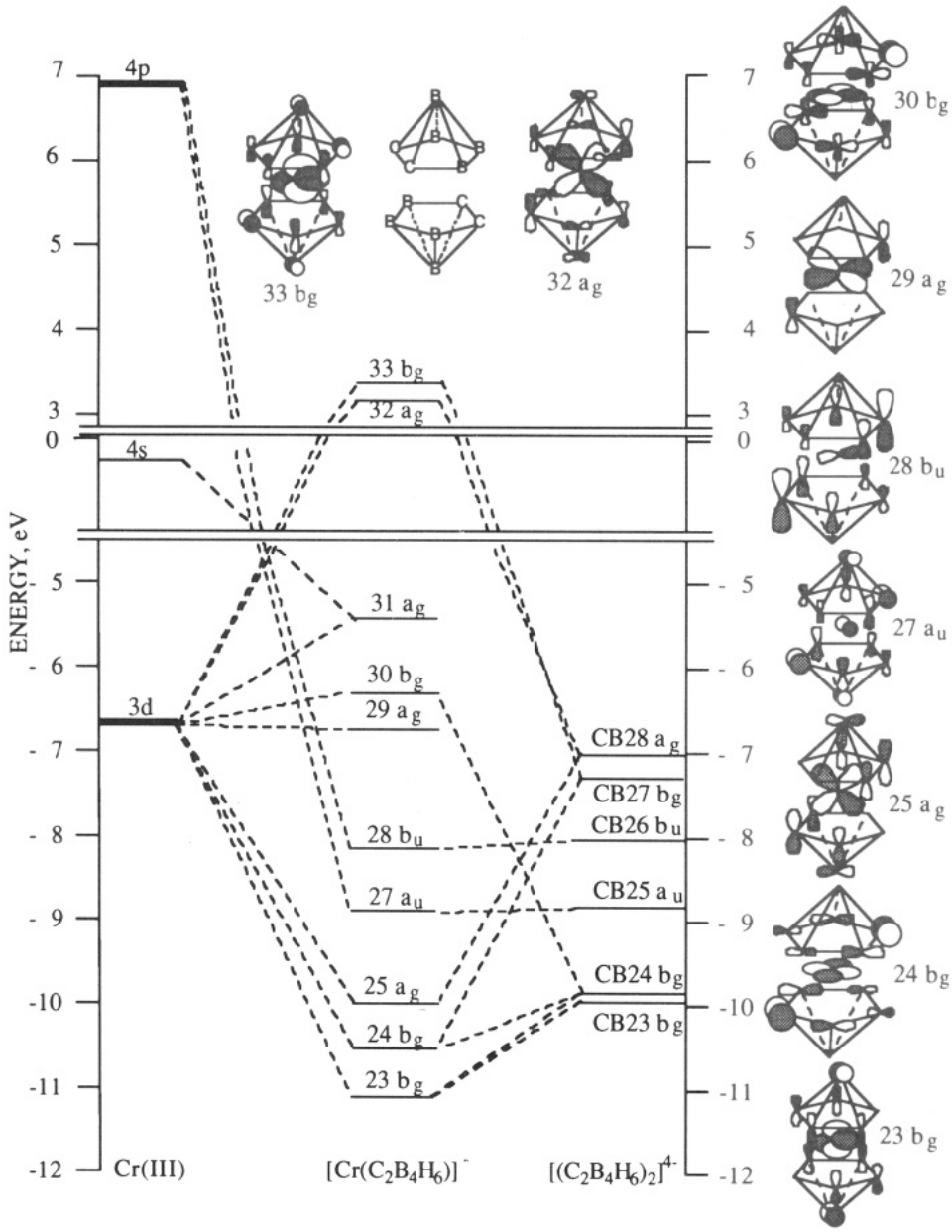

Figure 6. Molecular orbital correlation diagram for IX in terms of its carborane and chromium fragments, and sketches giving the heavy atom composition of some selected molecular orbitals.

Table IV shows that the chromium in VII is not symmetrically bonded to the C_2B_3 atoms of the carboranes, but is slightly dislocated, or slipped, toward the cage carbons. This slippage produces Cr–C(cage) distances that are about 0.14 Å shorter than the average Cr–B distances. Although the experimental indeterminations in IV and VI tend to mask any differences in the analogous bond lengths, the bond distances listed in Table IV suggest a similar slip distortion is occurring in these complexes as well. Although slip distortion is a common facet of main group metallacarborane sandwich complexes[7,41,42] and is found in the electron-rich transition metal carborane compounds,[43] it is invariably toward the boron side of the C_2B_3 face. A correlation between the extent of such a slippage and a folding of the C_2B_3 ring [so that the unique boron, B(4) in Figures 1–4, is below the B(3)–C(2)–C(1)–B(5) plane] has long been noted for both the icosahedral and pentagonal bipyramidal transition metal and main group metallacarboranes.[43b,44,45] Colquhoun, Greenhough, and Wallbridge[44] qualitatively explained the ring folding–slip distortion correlation found for the transition metal complexes in terms of metal d orbital–carborane interactions. However, the presence of a similar correlation in main group complexes indicates that additional factors are also important. While, at present, there is no good general explanation for this structural relationship, it is interesting to note that no ring folding was found in IV, VI, or VII. The C_2B_3 faces are planar within experimental error, indicating that metal slippage toward the carbons exerts a different influence on the carborane's geometry than does slippage toward the borons.

(40) Gard, E.; Haaland, A. *J. Organomet. Chem.* **1975**, *88*, 181.
(41) Islam, M. S.; Siriwardane, U.; Hosmane, N. S.; Maguire, J. A.; de Meester, P.; Chu, S. S. C. *Organometallics* **1987**, *6*, 1936.
(42) Siriwardane, U.; Islam, M. S.; West, T. A.; Hosmane, N. S.; Maguire, J. A.; Cowley, A. H. *J. Am. Chem. Soc.* **1987**, *109*, 4600.
(43) (a) Mingos, D. M. P.; Forsyth, M. I.; Welch, A. J. *J. Chem. Soc., Chem. Commun.* **1977**, 605. (b) Mingos, D. M. P.; Forsyth, M. I.; Welch, A. J. *J. Chem. Soc., Dalton Trans.* **1978**, 1363, and references therein.
(44) Colquhoun, H. M.; Greenhough, T. J.; Wallbridge, M. G. H. *J. Chem. Soc., Dalton Trans.* **1985**, 761.
(45) Hosmane, N. S.; Zhang, H.; Lu, K.-J.; Maguire, J. A. *Struct. Chem.* **1992**, in press.

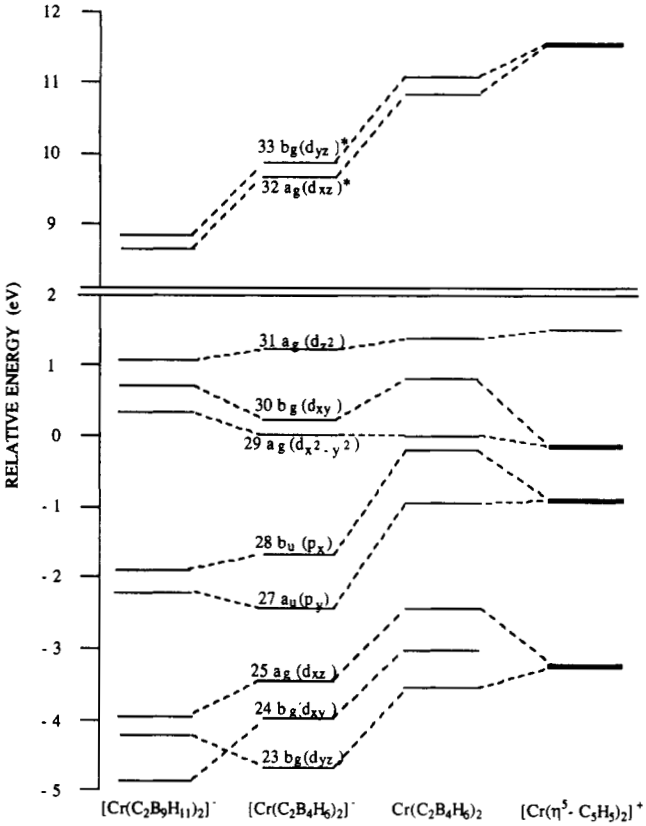

Figure 7. Energies of some molecular orbitals of $[Cr(C_2B_9H_{11})_2]^-$, IX, X, and VIII, relative to their input d orbitals.

The general structural features of the chromacarboranes (IV, VI, and VII) can be understood, at least in part, by Fenske–Hall molecular orbital analyses of the model complexes, 1,1′-*commo*-Cr[2,3-$C_2B_4H_6]_2^-$ [n = −1 (IX), 0 (X)]. Figure 6 shows the molecular orbital correlation diagram for the major chromium containing molecular orbitals (MO's) of IX in terms of the Cr(III) and $[(C_2B_4H_6)_2]^{4-}$ fragments. The figure also shows sketches of the relevant MO's, in terms of the valence atomic orbitals of the input atoms. Supplementary Table S-5 gives the percent atomic orbital compositions of the molecular orbitals of IX. The correlation diagram and orbital sketches are also qualitatively correct for X. Figure 7 shows the changes in the energies of these MO's in going from IX to X and also the relative energies of the analogous MO's of $[Cr(C_2B_9H_{11})_2]^-$ and chromocene, $[(\eta^5\text{-}C_5H_5)_2Cr]^+$ (VIII).[46] In the calculations, a coordinate system was defined such that the mirror plane of the $Cr(C_2B_4)_2$ cage was the *xz* plane and the unique boron, B(4) in Figures 1–4, was on the *x* axis. The HOMO of the $[(C_2B_4H_6)_2]^{4-}$ fragment is CB28a$_g$, therefore, the metal d^n electrons in IX and X will fill the molecular orbitals beginning with MO 29a$_g$. As can be seen from Figure 6, the main bonding interactions between the chromium and the carborane ligands arise primarily through MO's 23b$_g$ and 25a$_g$, followed by 24b$_g$. MO 23b$_g$ is localized on the chromium [24.7% Cr(d$_{yz}$), 7.0% B(3,5)(p$_z$), and 5.5% C(1,2)(p$_z$)] (see Figure 1 for the atom numbering system), while MO 25a$_g$ is also localized on the chromium, [24.7% Cr(d$_{xz}$), 5.6% C(1,2)(p$_z$), and 7.0% B(3,5)(p$_z$)]. Molecular orbital 24b$_g$, which contains 20.0% Cr(d$_{xy}$), is composed of a carborane atom orbitals that are directed primarily

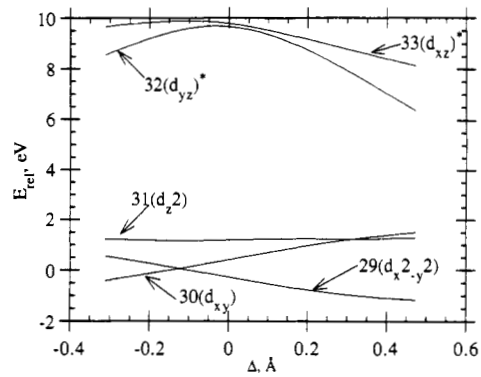

Figure 8. Plots of energy versus Δ for selected orbitals of IX. Δ = the lateral displacement, in Å, of the metal from the normal line drawn from the C_2B_3 bonding face of the carborane to the apical boron.

in the plane of the C_2B_3 face [13.5% B(4)(p$_y$) and 5.9% B(3,5)(p$_x$)]. Given these orbital compositions, it is not surprising that MO's 23b$_g$ and 25a$_g$ are the primary chromium–carborane bonding orbitals; their corresponding low-energy antibonding orbitals, 32a$_g$ and 33b$_g$, would be occupied in complexes with metals contributing more than six d electrons. The next set of MO's is composed of 27a$_u$ and 28b$_u$, which arise from very weak interactions between the Cr(4p) orbitals and the carborane fragment orbitals CB25a$_u$ and CB26b$_u$ [MO 27a$_u$ is 96.4% CB25a$_u$ and 28b$_u$ is 95.4% CB26b$_u$]. From Figure 6 it is apparent that Cr (p) bonding contributes little to the stability of the complex, both 27a$_u$ and 28b$_u$ could be treated as nonbonding molecular orbitals. This is quite different from the situation found in the main group metallacarborane complexes where metal p orbital–carborane interactions account for most of the metal–carborane bonding.[47] The electron counts in the complexes are such that the metal d^n electrons are distributed in MO's beginning with 29a$_g$, 30b$_g$, and 31a$_g$. These are metal-centered orbitals [29a$_g$ is 84.5% Cr(d$_{x^2-y^2}$) and 8.5% CB31a$_g$ (not shown); 30b$_g$ is 66.7% Cr(d$_{xy}$), 22.3% CB24b$_g$, and 9.4% CB29b$_g$; and 31a$_g$ is 90.5% Cr(d$_{z^2}$) and 3.9% Cr(4s)] whose energies are close to that of the input Cr(d) orbitals. A Fenske–Hall calculation, carried out on the bis(trimethylsilyl)-substituted chromacarborane (IV) yielded essentially the same results as those shown in Figures 6 and 7. That is, the metal bonds to the carborane mainly with its d$_{xz}$ and d$_{yz}$ orbitals, and the metal d^3 electrons are distributed in MO's almost identical to, and at the same relative energies as, MO's 29a$_g$, 30b$_g$, and 31a$_g$. Since the MO's of the model compounds, IX and X, are simpler than the SiMe$_3$-substituted ones, and the calculations required less time, bonding will be discussed in terms of the results on the model compounds.

The results shown in Figure 6 differ somewhat from the extended Hückel calculation results obtained by Mingos and co-workers,[7] on the sandwich complex, $[Cu(B_{11}H_{11})_2]^{n-}$. These investigators found that the energy of the orbitals equivalent to MO's 29a$_g$, 30b$_g$, and 31a$_g$ fell below the energies of 28b$_u$ and 27a$_u$ and attributed this ordering to the lower electronegativity of boron as compared to carbon and the choice of copper as the central atom. Figure 7 shows that, for the icosahedral and pentagonal-bipyramidal chromacarboranes, the MO orderings are more similar to that found in the chromocene complex than in the metallaboranes. However, our results agree with those of Mingos in that both calculations show that, in complexes with metals containing more than 6 d electrons, a slip

(46) The heavy atom geometry of the icosahedral chromacarborane was taken from ref 37 and the relative hydrogen positions were the MNDO-optimized positions for $Si(C_2B_9H_{11})_2$ from ref 47.

(47) Maguire, J. A. *Organometallics* **1991**, *10*, 3150.

distortion of the metal should greatly stabilize the complex.[7] This can be seen in Figure 8, which shows the change in the energies of the most geometrically sensitive MO's of IX, relative to the energies of the input metal d orbitals, as a function of Δ, the displacement of the metal from the normal drawn from the C_2B_3 plane to apical boron [B(6) in Figures 1–4].[48] As can be seen in Figure 8, a displacement of the metal toward the boron strongly stabilizes MO $32a_g$ by transforming the Cr–carborane interaction from antibonding to nonbonding. Although simple electron-rich commo complexes in the pentagonal bipyramidal system have yet to be structurally characterized, one would expect them to have the same slipped configuration as found in the electron-rich icosahedral metallacarboranes.[5,7]

Magnetic moment measurements of IV indicate three unpaired electrons and a $...(29a_g)^1(30b_g)^1(31a_g)^1$ electronic configuration. Although these three highest energy occupied MO's contribute little to the stability of the complex (see Figure 6), they exert an influence on the position of the chromium relative to the C_2B_3 ring atoms. One of the unusual structural features of IV, VI and VII is that the chromiums are not symmetrically bonded to the C_2B_3 atoms of the carborane face, but seem to be slipped toward the cage carbons. Figure 8 shows the relative energies of these MO's a function of Δ.[48] This figure shows that, at least for small values of Δ, the energy of MO $31a_g$ is essentially independent of Δ, while both MO $30b_g$ and $29a_g$ show significant energy changes. Indeed, these latter two orbitals show much larger energy variations with Δ than do any of the other MO's given in Figure 6. Molecular orbital $29a_g$, in which the chromium and B(4) are weakly bonding, decreases in energy as Δ increases, while the energy of MO $30b_g$, where the chromium and B(4) are antibonding, changes in the opposite way (see Figures 6 and 8). The two orbitals cross in energy at approximately Δ = −0.1 Å, which is close to the experimental value of −0.06 Å. Therefore, it is an open question as to the ordering of these two MO's in a specific complex; whatever the sequence, they are very close in energy. Because of the compensating energy changes on slippage of the metal that is found in $29a_g$ and $30b_g$ (see Figure 8), it is apparent that, at least until MO $32a_g$ is occupied, the driving force for slip distortion, either toward the cage carbons or the boron atoms, is small and only small dislocations of the metal would be expected. For IV and VI, it seems that the stabilization of MO $30b_g$ results in a slight slippage toward the cage carbons.

Although the above theoretical analyses are useful in rationalizing the structure and magnetic features of the Cr(III) complexes (compounds IV and VI), they cannot be as readily applied to VII. Comparison of the analogous bond distances in IV and VII, given in Table IV, shows that the oxidation of the Cr(III) to Cr(IV) produces no discernable structural effect. The magnetic susceptibility measurements on VII, coupled with the fact that acceptable NMR spectra could be obtained for this compound, indicate a diamagnetic complex. Oxidation of IV to VII would require the removal of the electron from MO $31a_g$, which is essentially the $Cr(3d_{z^2})$ orbital. This should not materially alter chromium–carborane bonding and the structural effects of a one electron oxidation of IV should be small. However, the fact that the structures of IV and VII are identical is somewhat surprising. Figure 7 shows that, as one goes from IX to X, there is an increase in the energy difference between MO $29a_g$ and MO $30b_g$. However, in view of the orbital energy separations calculated in the paramagnetic Cr(III) species IX, $[Cr(C_2B_9H_{11})_2]^-$, and $[(\eta^5\text{-}C_5H_5)_2Cr]^+$ (VIII), also shown in Figure 7, it is difficult to rationalize, at least on the basis of Fenske–Hall calculations, how depopulation of MO $31a_g$ could induce spin pairing in the two lower energy orbitals. Xα-scattered wave SCF molecular orbital calculations[49] on IX and X showed essentially the same results as did the Fenske–Hall calculations, that is, in both IX and X the metal d electrons are distributed in a set of three closely spaced metal-centered MO's very similar to MO's $29a_g$, $30b_g$, and $31a_g$.[50]

One other possibility is that of a singlet...$(29a_g)^1(30b_g)^1$ configuration. This could arise from an unusually large zero-field splitting in the triplet state, or by some other interaction. Such a configuration would be more consistent with the MO analysis. However, it is not apparent how such interactions could arise. The unit cell of VII (not shown) consists of four molecules that are well separated, with the shortest Cr–Cr distance being 9.851 Å. Therefore, it seems unlikely that intermolecular interactions could be an important factor.

Since compound VII is the first reported π complex of Cr(IV), there are not analogous complexes that can be used for comparison. In general, very little information is available on the structure and properties of electron deficient ($<d^6$) metallacarboranes. The Cr(III) complexes have been the most extensively studied. Hawthorne and co-workers have reported the synthesis,[4] electrochemical behavior,[51] and magnetic properties[52] of $[Cr^{III}(C_2B_9H_{11})_2]^-$. The structure of the bis(methyl) derivative, $\{Cr^{III}[(CCH_3)_2B_9H_9]_2\}^-$ has also been reported.[37] In these chromacarboranes, the chromium, in a formal 3+ oxidation state, is centered above the pentagonal faces of the carborane ligands, the complexes are paramagnetic with three unpaired electrons, and show no reversible waves in their cyclic voltammograms. These properties are very similar to those of IV and VI as would be expected from the similarities in their electronic structure as exhibited in Figure 7. Salentine and Hawthorne have reported the synthesis and properties of a number of electron-deficient supraicosahedral sandwich complexes of the form $[M^{II}(C_2B_{10}H_{12})_2]^{2-}$ (M = Ti, V, Cr, and Mn).[51] The structure of the titanium complex, $\{Ti[1,6\text{-}(CCH_3)_2B_{10}H_{10}]_2\}^{2-}$, showed that the complex consists of two closed 13-vertex polyhedra that share a common Ti vertex.[53] The hexagonal C_2B_4 bonding face of the carborane is not planar and the titanium is not symmetrically bonded to these atoms. However, the different bond distances seem to be more a result of the nonplanarity of the carborane bonding face than a slip distortion of the metal. Similarities in the spectra of the complexes indicate that this structure is common to the series. Magnetic measurements showed zero, one, two, and one unpaired electron for M = Ti(d^2), V(d^3), Cr(d^4), and Mn(d^5), respectively.[53] These results are consistent with a MO sequence of one low-energy MO and two closely spaced, or degenerate, higher energy MO's in which the metal electrons are distributed. This sequence is the reverse of that found in the pentagonal bipyramidal chromacarboranes and chromocene (see Figure

(48) Δ is the latteral displacement of the metal from the extension of the C_2B_3–B(6) normal. For reference, Δ for C(1,2) = −1.10 Å, B(3,5) = 0.355 Å, and B(4) = 1.39 Å.

(49) (a) Slater, J. C. *Adv. Quantum Chem.* **1972**, *6*, 1. (b) Johnson, K. H. *Adv. Quantum Chem.* **1973**, *7*, 143. (c) Johnson, K. H. *Annu. Rev. Phys. Chem.* **1975**, *26*, 39.

(50) Maguire, J. A. Unpublished results.

(51) Salentine, C. G.; Hawthorne, M. F. *Inorg. Chem.* **1976**, *15*, 2872.

(52) Crawford, V. H.; Hatfield, W. E.; Salentine, C. G.; Callahan, K. P.; Hawthorne, M. F. *Inorg. Chem.* **1979**, *18*, 1600.

(53) Lo, F. Y.; Strouse, C. E.; Callahan, K. P.; Knobler, C. B.; Hawthorne, M. F. *J. Am. Chem. Soc.* **1975**, *97*, 428.

7). To date, the results indicate that carborane ligands tend to stabilize electron-deficient complexes of high oxidation state much more so than do cyclopentadienides. However, there is not as yet sufficient experimental or theoretical results to provide a basis for understanding of the factors that dictate the stabilities and properties of these complexes. Further studies are currently underway in our laboratories.

Acknowledgment. This work was supported by grants from the National Science Foundation (CHE-9100048 to NSH), the Robert A. Welch Foundation (N-1016 to NSH), and the donors of the Petroleum Research Fund, administered by the American Chemical Society (to N.S.H. and J.A.M.). The help and assistance of Dr. R. L. Cerny and Mr. C. Jacoby of the Midwest Center for Mass Spectrometry, a National Science Foundation Regional Instrumentation Facility (grant no. CHE-8211164), is gratefully acknowledged. This research was also supported in part by grant from the Office of Naval Research (to W.E.H.).

Supplementary Material Available: Listings of mass spectrometric data (Table S-1) of IV–VII, a table of bond angles (Table S-2), a table of anisotropic displacement coefficients of IV, VI, and VII (Table S-3), a table of H-atom coordinates and isotropic displacement coefficients of IV, VI, and VII (Table S-4), and a table of the atomic orbital compositions of the molecular orbitals of IX (Table S-5) (14 pages). Ordering information is given on any current masthead page.

OM920383C

Addition of Aldehydes to Tantalum–Carbene Complexes and the Reduction of Epoxides by Unsaturated Tantalum Complexes. Theoretical Study of the Reaction Mechanism and Product Structures

Birgit Schiøtt* and Karl Anker Jørgensen

Department of Chemistry, Aarhus University, DK-8000 Aarhus C, Denmark

Maria José Calhorda* and Adelino M. Galvão†

Centro de Tecnologia Química e Biológica, Apartado 127, 2780 Oeiras, Portugal, and Departamento de Engenharia Química, Instituto Superior Técnico, 1096 Lisboa Codex, Portugal

Received April 10, 1992

The addition of formaldehyde to $Cp_2Ta(CH_3)(CH_2)$ is studied from a molecular orbital point of view. Two possible isomers of the product, O-*anti*-$Cp_2(CH_3)\overline{Ta(OCH_2CH_2)}$ and O-*syn*-$Cp_2(CH_3)\overline{Ta(OCH_2CH_2)}$, are analyzed. The anti isomer is suggested to be thermodynamically more stable because it has stronger tantalum–carbon bonds. Steric hindrance of the Cp rings may result in the initial formation of the syn isomer only. Different routes for the following rearrangement to the anti isomer are compared. Berry pseudorotation and turnstile rotations are both high-energy processes. Methyl migration via one of the Cp rings is a possible pathway from energetic and bonding considerations. This reaction path is found to be base catalyzed. The possibility of an acid-catalyzed heterolysis of the tantalum–oxygen bond is discussed. The reduction of ethylene oxide by a $Cp_2Ta(CH_3)$ complex is also studied. A direct oxygen abstraction pathway is compared to one involving the formation of the tantalaoxetanes $Cp_2(CH_3)\overline{Ta(OCH_2CH_2)}$. An initial weak coordination of the epoxide through the oxygen atom is suggested. A concerted elimination of the alkene from this precursor is a nonactivated process, opposed to a path that involves formation of tantalaoxetanes by an insertion of tantalum into a carbon–oxygen bond of the epoxide.

The existence of metallaoxetanes as intermediates in various transition-metal-catalyzed oxygen-transfer reactions, such as alkene epoxidation,[1] epoxide reduction,[2] Tebbe-like reactions,[3] and insertion of carbon dioxide into epoxides,[4] has been a subject of intense debate during the past two decades.[5] Reports dealing with theoretical aspects of the chemistry of transition-metal metallaoxetanes have appeared in the literature.[6] This report will discuss the formation of tantalaoxetanes in two of the above reaction types, namely, in the Tebbe-like reaction of a tantalum–carbene complex with aldehydes and in the reduction of epoxides by a tantalum complex. The extended Hückel method[7] is applied throughout the study.

Table I. Atomic Parameters

atom	orbital	H_{ij}, eV	ζ_1	ζ_2	c_1[a]	c_2[a]
Ta	6s	−10.10	2.280			
	6p	−6.86	2.241			
	5d	−12.00	2.762	1.938	0.6600	0.5592
O	2s	−32.20	2.275			
	2p	−14.80	2.275			
C	2s	−21.40	1.625			
	2p	−11.40	1.625			
H	1s	−13.60	1.300			

[a] Coefficients used in a double-ζ expansion of the metal d-orbitals.

The Tebbe-like reaction is the organometallic analogue

† Only Instituto Superior Técnico.

0276-7333/92/2311-4213$03.00/0